

# 1 **A wheat kinase and immune receptor form the host-specificity** 2 **barrier against the blast fungus**

3 Sanu Arora<sup>1,8</sup>, Andrew Steed<sup>1,8</sup>, Rachel Goddard<sup>1,8</sup>, Kumar Gaurav<sup>1,8</sup>, Tom O'Hara<sup>1,8</sup>, Adam  
4 Schoen<sup>3</sup>, Nidhi Rawat<sup>3</sup>, Ahmed F. Elkot<sup>5</sup>, Catherine Chinoy<sup>1</sup>, Martha H. Nicholson<sup>1</sup>, Soichiro  
5 Asuke<sup>4</sup>, Burkhard Steuernagel<sup>1</sup>, Guotai Yu<sup>1</sup>, Rajani Awal<sup>1</sup>, Macarena Forner-Martínez<sup>1</sup>,  
6 Luzie Wingen<sup>1</sup>, Erin Baggs<sup>6</sup>, Jonathan Clarke<sup>1</sup>, Ksenia V. Krasileva<sup>6</sup>, Yukio Tosa<sup>4</sup>, Jonathan  
7 D. G. Jones<sup>2</sup>, Vijay K. Tiwari<sup>3</sup>, \*Brande B. H. Wulff<sup>1,7</sup>, \*Paul Nicholson<sup>1</sup>

8 <sup>1</sup>John Innes Centre, Norwich Research Park, Norwich, UK.

9 <sup>2</sup>The Sainsbury Laboratory, Norwich Research Park, Norwich, UK.

10 <sup>3</sup>Department of Plant Science and Landscape Architecture, University of Maryland, College  
11 Park, MD 20742, United States.

12 <sup>4</sup>Graduate School of Agricultural Science, Kobe University, Kobe 657-8501, Japan.

13 <sup>5</sup>Wheat Research Department, Field Crops Research Institute, Agricultural Research Center,  
14 12619, Giza Egypt.

15 <sup>6</sup>Department of Plant and Microbial Biology, University of California, Berkeley, California  
16 94720, USA.

17 <sup>7</sup>Present address: Center for Desert Agriculture, Biological and Environmental Science and  
18 Engineering Division (BESE), King Abdullah University of Science and Technology  
19 (KAUST), Thuwal 23955-6900, Saudi Arabia.

20 <sup>8</sup>These authors contributed equally.

21 \*Correspondence should be addressed to PN ([paul.nicholson@jic.ac.uk](mailto:paul.nicholson@jic.ac.uk)) or BBHW  
22 ([brande.wulff@kaust.edu.sa](mailto:brande.wulff@kaust.edu.sa))

## 23 **Abstract**

24 Since emerging in Brazil in 1985, wheat blast has spread throughout South America and  
25 recently appeared in Bangladesh and Zambia. We show that two wheat resistance genes,  
26 *Rwt3* and *Rwt4*, acting as host-specificity barriers against non-Triticum blast pathotypes  
27 encode a nucleotide-binding leucine-rich repeat immune receptor and a tandem kinase,  
28 respectively. Molecular isolation of these genes allowed us to develop assays that will ensure  
29 the inclusion of these two genes in the wheat cultivars to forestall the recurrence of blast host  
30 jumps.

31

32

### 33 **Main**

34 The occurrence of pathogen host jumps suggests that seemingly durable non-host resistance  
35 can be fragile<sup>1</sup>. This is illustrated by the jump of the blast fungus (*Pyricularia oryzae*, syn.  
36 *Magnaporthe oryzae*) from ryegrass to wheat in Brazil in 1985<sup>2</sup>. The pathogen subsequently  
37 spread to cause epidemics in other regions of Brazil and neighbouring countries including,  
38 Bolivia and Paraguay<sup>3</sup>. Outbreaks of wheat blast occurred in Bangladesh in 2016 and the  
39 disease was reported from Zambia in 2018<sup>4,5</sup>. Wheat blast is now considered to pose a threat  
40 to global wheat production<sup>6</sup>, and discovery and deployment of resistance genes against this  
41 pathogen are critical to mitigate its threat.

42 While *Pyricularia oryzae* exhibits a high level of host specificity, *Triticum* pathotypes are  
43 closely related to *Lolium* and *Avena* pathotypes<sup>7</sup>. Two pathogen genes, *PWT3* and *PWT4*,  
44 condition avirulence of *Avena* pathotypes on wheat (*Triticum aestivum*) while *PWT3* prevents  
45 infection of wheat by *Lolium* pathotypes<sup>8,9</sup>.

46 The resistance genes *Rwt3* and *Rwt4* in wheat recognise respectively the *PWT3* and *PWT4*  
47 avirulence gene products to prevent infection. It has been proposed that the epidemics in  
48 Brazil occurred due to the widespread cultivation of varieties lacking *Rwt3* that are  
49 susceptible to *Lolium* pathotypes<sup>7</sup>. *Lolium* pathotypes have also been associated with the  
50 occurrence of wheat blast in the USA<sup>10,11</sup>. These reports emphasize the importance of  
51 maintaining *Rwt3* and *Rwt4* in wheat cultivars to prevent future host jumps of the *Avena*,  
52 and/or *Lolium* pathotypes.

53 To identify candidates for *Rwt3* and *Rwt4*, we used a Triticeae bait library (Table S1,  
54 Additional File F1) to capture and sequence the NLR complements of 320 wheat lines  
55 including 300 wheat landraces from the A.E. Watkins collection harbouring the genetic  
56 diversity existing prior to intensive breeding (Table S2, Supplementary Fig. 1). We screened  
57 seedlings of the panel with Br48, a *Triticum* pathotype of *Pyricularia oryzae*, transformed  
58 with either *PWT3* or *PWT4*<sup>7</sup> (Table S3; Supplementary Fig. 2, 3) and performed *k*-mer based  
59 association genetics. This led to an identification of candidate NLR genes for *PWT3* and  
60 *PWT4* recognition (Fig 1a-b, Supplementary Fig. 4, Supplementary Fig. 11) on chromosome  
61 1D within the mapping intervals of *Rwt3* and *Rwt4*, respectively<sup>9,12</sup>.

62 Investigating the presence of these candidate genes in the NLR assemblies of *Aegilops*  
63 *tauschii*<sup>13</sup>, the D-genome progenitor of bread wheat, the *Rwt4* candidate was found only in  
64 lineage 2 (L2) while the *Rwt3* candidate was found only in lineage 1 (L1) (Table S4,

65 Supplementary Fig. 5). This explains why we could identify only the *Rwt4* candidate, and not  
66 the *Rwt3* candidate, by phenotyping and performing association genetics on an NLR gene  
67 enrichment-sequenced *Ae. tauschii* L2 panel<sup>13</sup> (Table S5, Supplementary Fig. 6, 7). The L2  
68 origin of *Rwt4* is consistent with L2 being the major contributor of the wheat D-genome,  
69 however, the L1 origin of *Rwt3* is more remarkable considering that the L1 signature in wheat  
70 is mostly concentrated around a 5 Mb region surrounding the *Rwt3* candidate<sup>14</sup>  
71 (Supplementary Fig. 8). This finding suggests that pathogen pressure could have played a  
72 significant role in post-domestication wheat evolution.

73 To functionally validate the *Rwt3* NLR candidate, we screened a TILLING population of  
74 Jagger<sup>15</sup> and found three lines each carrying a functional mutation in this gene  
75 (Supplementary Fig. 9). One line, M217, is homozygous for a mutation causing a premature  
76 stop codon whereas another, M698, is homozygous for a mis-sense mutation (G241E)  
77 predicted to cause functional aberration in the protein (Fig. 1c, Table S6). In both the leaf and  
78 head assays of these mutants using Br48+*PWT3*, a loss of the wildtype resistance was  
79 observed (Fig. 1d-e). The third line, M1164, is heterozygous for another deleterious mis-  
80 sense mutation (E492K) (Fig. 1c, Table S6). In both the leaf and head assays of the  
81 segregating progeny of M1164 using Br48+*PWT3*, those homozygous for the mutation were  
82 found to be susceptible while the others were resistant (Fig 1d-e, Supplementary Fig. 10).  
83 The clear loss of function observed in three independently derived TILLING mutants and the  
84 co-segregation of the M1164 mutation with susceptibility shows that the *Rwt3* NLR candidate  
85 is required for resistance to *P. oryzae* expressing the *PWT3* effector.

86 We observed that the identified *Rwt4* NLR candidate is adjacent to an allele of a wheat  
87 tandem kinase (WTK) previously reported to confer resistance against powdery mildew<sup>16</sup>.  
88 The 532 kb mapping interval of powdery mildew resistance contained an allele of the *Rwt4*  
89 NLR candidate identified in our study, in addition to the WTK. On functional testing by Lu et  
90 al (2020)<sup>16</sup>, the WTK, and not the NLR, was found to be necessary and sufficient to confer  
91 resistance to powdery mildew and was designated as *Pm24*. Therefore, we tested both the  
92 identified *Rwt4* NLR candidate (Supplementary Fig. 11) and the linked *Pm24* allele  
93 (Supplementary Fig. 12) as candidates for *Rwt4* using the Cadenza TILLING resource<sup>17</sup>. For  
94 the NLR candidate, we identified four lines (two heterozygous and two homozygous)  
95 carrying mutations predicted to cause premature stop codons and six additional lines (four  
96 heterozygous and two homozygous) carrying mis-sense mutations predicted to have a  
97 significant impact on tertiary structure (Table S6). Neither the homozygous nor any progeny

98 of the heterozygous mutants for this candidate showed an increase in susceptibility relative to  
99 the wildtype Cadenza in either leaf or head assays with Br48+*PWT4* (Supplementary Fig.  
100 13). For the linked *Pm24* allele, we tested three lines (one homozygous and two  
101 heterozygous) carrying mutations that result in premature stop codons (Table S6). In both the  
102 leaf and head assays of the homozygous line M0159 using Br48+*PWT4*, a clear increase in  
103 susceptibility compared to the wildtype was observed (Fig. 1g-h). In the leaf and head assays  
104 of the segregating progeny of heterozygous mutants (M0971 and M1103) using Br48+*PWT4*,  
105 those homozygous for the mutation were found to be susceptible while all others were  
106 resistant (Supplementary Fig. 14). These results show that as in the case of *Pm24*, the linked  
107 WTK, and not the identified NLR candidate, is required for resistance to *P. oryzae* expressing  
108 the *PWT4* effector. The finding that WTK alleles, *Pm24* and *Rwt4*, are involved in resistance  
109 to two unrelated fungal pathogens suggests that it may be a broad-spectrum component of  
110 disease resistance.

111 We developed KASP markers for *Rwt3* and *Rwt4* (Table S7) and validated them on the core  
112 300 Watkins accessions (Table S8). *Rwt3* is present only in 145 of the 193 Watkins  
113 accessions resistant to Br48+*PWT3* (Fig. 2a, Table S8), while *Rwt4* is present only in 136 of  
114 the 270 Watkins accessions resistant to Br48+*PWT4* (Fig. 2b, Table S8). This suggests that  
115 there are other resistance genes in the Watkins panel recognising *PWT3*, *PWT4* or additional  
116 effectors in Br48. We re-ran GWAS with the leaf assay disease phenotype of Br48+*PWT4*,  
117 restricted to the Watkins lines not containing *Rwt4*. Using Jagger as the reference genome, we  
118 obtained a clear peak on chromosome 1B in the region homeologous to that on 1D containing  
119 *Rwt4* (Fig. 2e), indicating that *Rwt4* has a homeologue on chromosome 1B that provides  
120 resistance to *P. oryzae* expressing the *PWT4* effector. We followed the same protocol and re-  
121 ran the GWAS with the leaf assay disease phenotype of Br48+*PWT3*, restricted to the  
122 Watkins lines not containing *Rwt3*. This identified a clear peak on chromosome 2A using  
123 Mattis as the reference genome (Fig. 2c) and another on chromosome 7A using Jagger as the  
124 reference genome (Fig. 2d). A resistance termed *Rmg2* located on chromosome 7A has  
125 previously been identified in the cultivar Thatcher<sup>18</sup> and a resistance termed *Rmg7* has been  
126 reported on the distal region of the long arm of chromosome 2A of tetraploid wheat<sup>19</sup>. In both  
127 instances the resistances were identified using the same isolate, Br48, as used in our work  
128 suggesting that the resistances identified on chromosomes 2A and 7A may correspond to  
129 *Rmg7* and *Rmg2* reported previously. Watkins lines carrying the 7A resistance showed  
130 similar levels of resistance to both Br48 and Br48+*PWT3* (Supplementary Fig. 15) indicating

131 that this resistance is due to interaction with Br48 and supporting its characterisation as  
132 *Rmg2*.

133 We designed a KASP-based marker for the *Rwt4* 1B homeologue (Tables S8, S9) which,  
134 along with those for *Rwt3* and *Rwt4*-1D, should enable wheat breeders to ensure that cultivars  
135 contain resistance effective against *PWT3* and *PWT4* and therefore maintain host-specificity  
136 barriers against *Lolium* and *Avena* pathotypes of *P. oryzae*. It was due to the lack of this  
137 information that *Rwt3* failed to make its way into elite cultivars such as Anahuac despite  
138 being widely present in wheat landraces (Table S9), which was the probable cause of the  
139 original wheat blast epidemic in Brazil (Fig. 3a). A future host jump of *P. oryzae* poses a high  
140 risk of host range expansion of *Triticum* pathotypes of *P. oryzae*. This risk was illustrated in  
141 the recent study of Inoue et al (2021)<sup>20</sup>, which showed that the resistance conferred by *Rmg8*  
142 is suppressed by *PWT4* and that the presence of *Rwt4* in wheat prevents this suppression.  
143 *Rmg8*, along with *Rmg7*, recognises the effector *AVR-Rmg8* and is one of the few reported  
144 resistances that show effectiveness against *Triticum* pathotypes of *P. oryzae* at both the  
145 seedling and head stage<sup>21</sup>. If *Triticum* pathotypes acquire *PWT4* from a future host jump, the  
146 resistance provided by *Rmg8* would be lost (Fig. 3b). Therefore, it is important to ensure the  
147 presence of *Rwt4* in wheat cultivars not only to prevent a future host jump but also to  
148 maintain the effectiveness of *Rmg8* against wheat blast if such an event occurs.

149

150

151

152

153

154

155

156

157

158

159

160

161

162

163

164

165

166

## 167 **Methods**

### 168 **Watkins panel configuration**

169 Using the SSR genotype data from Wingen et al (2014)<sup>22</sup>, a core set of 300 genetically  
170 diverse wheat landraces with spring growth habit were selected from the Watkins collection  
171 (Supplementary Fig. 1, Table S2) along with 20 non-Watkins lines. The DNA was extracted  
172 following a modified CTAB protocol<sup>23</sup>. The seeds of these lines are available from the  
173 Germplasm Resources Unit ([www.seedstor.ac.uk](http://www.seedstor.ac.uk)) under Wheat Resistance gene enrichment  
174 (WREN) sequencing collection (WREN0001- WREN0320).

### 175 **Phenotyping of *Ae. tauschii* and Watkins panels with wheat blast isolates**

176 The *M. oryzae* pathotype *Triticum* (MoT) isolate Br48 and the transformed isolates  
177 Br48+PWT3 and Br48+PWT4<sup>7</sup> were grown on complete medium agar (CMA). A conidial  
178 suspension of 0.3 – 0.4 x10<sup>6</sup> conidia per ml was used for all inoculations. Detached seedling  
179 assays with the *Ae. tauschii* and Watkins panels were carried out as described by Goddard et  
180 al (2020)<sup>24</sup> and scored for disease symptoms using a 0 – 6 scale (Supplementary Fig. 2, 3 and  
181 6; Table S3, S5). Resistance at the heading stage was assessed according to Goddard et al  
182 (2020)<sup>24</sup>. Heads of *Ae. tauschii* and wheat were scored using a 0 – 6 scale (Supplementary  
183 Fig. 2e and 2f, respectively).

### 184 **Bait library design for the Watkins panel**

185 Two bait libraries were used for the capture of the immune receptors from the Watkins panel  
186 (i) NLR Triticeae bait library V3 (<https://github.com/steuernb/MutantHunter/>), including 275  
187 genes conserved in grasses<sup>25</sup> and (ii) A new bait library which included NLRs extracted from  
188 the genomes of *T. turgidum* cv. Svevo and cv. Kronos and *T. dicoccoides* cv. Zavitan and  
189 only those genes that had <50% coverage by previously designed baits were used. To remove  
190 redundancies, NLR sequences were passed through CD-HIT (v4.6.8-2017-0621 -c 0.9 -G 0 -  
191 aS 0.9 -p 1). This bait design also included wheat domestication genes *VRN1A* (AY747598),  
192 *Wx1* (AY050174), *Q* (AY702956), *Rht-b1* (JX993615), *Rht-d1* (HE585643), *NAM-B1*  
193 (MG587710) as well as wheat orthologs of known immune signalling components ICS1,  
194 NPR1, NDR1, EDS1, PAD4, SRFR1, SAG101, RAR1, SGT1, HSP90.2, HSP90.4, RIN4,  
195 ADR1 and PBS1 extracted through BioMart (Table S1, Additional File 1). The bait probes  
196 were designed by Arbor Bioscience and filtered with their Repeat Mask pipeline which



197 removed the baits that were >50% Repeat Masked and any non-NLR baits with >3 hits in the  
198 wheat genome. To balance for the low copy number genes, baits derived from domestication  
199 genes were multiplied 10x and those derived from immune signalling genes were 3x  
200 compared to the baits derived from NLRs.

### 201 **Library construction and sequencing of the Watkins panel**

202 Illumina libraries with an average insert size of 700 bp were enriched by Arbor Biosciences,  
203 Michigan, USA, as previously described<sup>26</sup>, and sequenced on an Illumina HiSeq with either  
204 150 or 250 PE reads at Novogene, China to generate an average of 3.82 Gb per accession  
205 (Table S2). The raw reads were trimmed using Trimmomatic v0.2<sup>27</sup> and *de novo* assembled  
206 with the CLC Assembly Cell (<http://www.clcbio.com/products/clc-assembly-cell/>) using  
207 word size (-w = 64) with standard parameters.

### 208 **Generating Watkins *k*-mer presence/absence matrix and its phylogeny**

209 A presence/absence matrix of *k*-mers ( $k = 51$ ) was constructed from trimmed raw data  
210 using Jellyfish<sup>28</sup> as described in Arora et al (2019)<sup>13</sup>. *k*-mers occurring in less than four  
211 accessions or in all but three or fewer accessions were removed during the construction of the  
212 matrix. From the *k*-mer matrix generated with Watkins RenSeq data, 5310 randomly  
213 extracted *k*-mers were used to build a UPGMA (unweighted pair group method with  
214 arithmetic mean) tree with 100 bootstraps.

### 215 ***k*-mer based association mapping**

216 For the reference genomes of *T. aestivum* - Chinese Spring<sup>29</sup>, Jagger and Mattis<sup>30</sup> – and of *Ae.*  
217 *tauschii* AY61<sup>31</sup>, NLRs were predicted using NLR-Annotator<sup>32</sup> and their sequences along  
218 with 3kb sequence from both upstream and downstream region (if available) were extracted  
219 using samtools (version 1.9) to create the corresponding reference NLR assemblies. The  
220 disease phenotypes were averaged across the replicates after removing the non-numerical  
221 values and the mean phenotype scores multiplied by -1 so that a higher value represents a  
222 higher resistance. For those *k*-mers of a reference NLR assembly whose presence/absence in  
223 the panel correlates with the phenotype, that is, the absolute value of Pearson's correlation  
224 obtained was higher than 0.1, a *p*-value was assigned using linear regression while taking the  
225 three most significant PCA dimensions as covariates to control for the population structure. A  
226 stringent cut-off of 8, based on Bonferroni-adjustment<sup>14</sup> to a *p*-value of 0.05, was chosen for  
227 Watkins RenSeq association mapping, while a cut-off of 7 was chosen for *Ae. tauschii* L2  
228 RenSeq association mapping (Supplementary Fig. 7).

### 229 ***In silico* gene structure prediction**

230 The *Rwt3* NLR candidate gene transcript is 5,937 bp. Only one of the 15 annotated exons  
231 (grey colored exon in Fig. 1c) appears to be translated into protein. This exon encodes a  
232 protein of 1069 amino acids with a coiled-coil domain, an NB-ARC domain and several  
233 leucine rich repeats (LRRs) motifs at the C-terminus (Supplementary Fig. 4). The *Rwt4* NLR  
234 candidate gene is 3,117 bp with three exons. The predicted protein of 1038 amino acids  
235 contain domains with homology to a coiled-coil (CC) domain, two NB-ARC domains and  
236 two LRR at the C-terminus (Supplementary Fig. 11). The *Rwt4* WTK candidate has an open  
237 reading frame of 2,751 bp which has eleven predicted exons that encode a protein of 916  
238 amino acids with putative tandem protein kinase domains (Fig. 1f; Supplementary Fig. 12).  
239 Domains were predicted by NCBI and Pfam databases. The gene structure of both *Rwt3* and  
240 *Rwt4* NLR candidate genes was consistent with that predicted using cDNA RenSeq data of  
241 Watkins lines.

#### 242 **Identification and phenotyping of Cadenza TILLING mutants to test the function of** 243 ***Rwt4***

244 Cadenza TILLING lines<sup>17</sup> for the NLR candidate for *Rwt4* were identified within the Plant  
245 Ensembl database for the gene TraesCS1D02G059000  
246 ([http://plants.ensembl.org/Triticum\\_aestivum/Gene/](http://plants.ensembl.org/Triticum_aestivum/Gene/)). Lines containing mutations leading to  
247 premature stop codons and those for which the 'sorting intolerant from tolerant' (SIFT) score  
248 was 0.0 or 0.01 were selected for phenotyping. For the *Rwt4* kinase candidate gene, Cadenza  
249 TILLING lines were identified for the gene TraesCS1D02G058900. Details of the mutations  
250 present in the Cadenza TILLING lines is provided in the Table S6.

#### 251 **Identification and phenotyping of Jagger TILLING mutants to test the function of *Rwt3***

252 For selecting mutations in the *Rwt3* candidate gene (TraesCS1D02G029900), TILLING was  
253 performed in wheat cultivar Jagger<sup>15</sup> using genome specific primer pairs (Supplementary Fig.  
254 9a-d). The effects of the mutations on the predicted protein were analysed using SnapGene®  
255 software (version 5.0.7 from GSL Biotech). The effects of missense mutations were  
256 determined using PROVEAN (Protein Variation Effect Analyzer) v1.1 software<sup>33</sup>. Selected  
257 lines were phenotyped as described above. Details of the mutations is provided in Table S6.

#### 258 **KASP analysis and sequencing of TILLING lines to confirm mutations**

259 Kompetitive Allele-Specific PCR (KASP) (LGC Genomics) was performed to confirm  
260 mutations where suitable PCR primers could be designed. Alternatively, the region  
261 containing the mutation was amplified and purified products were sequenced by Eurofins  
262 Genomics. Sequence analysis was performed with Geneious Prime software.

#### 263 **Anahuac DNA preparation, sequencing, and assembly to check presence of *Rwt3* gene**



264 To confirm that Anahuac is a non-carrier of *Rwt3*, we captured its NLR complement using  
265 the bait libraries described above. The *Rwt3* NLR candidate was absent in the CLC assembly  
266 generated as described above.

### 267 **KASP marker design to detect *Rwt3* and *Rwt4* in wheat cultivars and Watkins collection**

268 The regions differentiating resistant and susceptible alleles of *Rwt4* from the *Ae. tauschii* L2  
269 panel were used to design KASP markers. The KASP marker discriminated between resistant  
270 and susceptible accessions in *Ae. tauschii* L2 panel but did not distinguish reliably between  
271 resistant and susceptible lines in the Watkins panel. The resistant allele of *Rwt4* was the same  
272 in both the *Ae. tauschii* L2 and the Watkins panels but the susceptible allele of *Rwt4* in the  
273 Watkins panel originated from *Ae. tauschii* L3 and not *Ae. tauschii* L2. This is consistent with  
274 the multi-lineage hybridisation hypothesis proposed in Gaurav et al 2021<sup>14</sup>. A new marker  
275 was designed by comparing the common resistant allele with susceptible alleles from both the  
276 *Ae. tauschii* L2 and Watkins panels (Table S7) that successfully distinguished between the  
277 resistant and susceptible alleles in the wheat lines (Table S8).

278 We used the D-genomes of 11 chromosome-scale wheat assemblies<sup>30</sup> to fetch the D-genome  
279 susceptible allele of *Rwt3* and designed KASP markers (Table S7). The marker distinguished  
280 resistant from susceptible lines and had a high correlation with presence-absence scored with  
281 *in silico* markers (Table S8). KASP markers were tested on the entire Watkins panel (~900)  
282 to understand the distribution of these genes in the landrace collection (Table S9).

### 283 **Characterisation of the resistance identified on chromosome 7A**

284 A set of Watkins lines were genotyped as carrying either *Rwt3* or the 7A resistance or having  
285 neither or both resistances. All accessions were phenotyped in leaf assays using isolates Br48  
286 and Br48+*PWT3*. Accessions lacking either resistance were susceptible to both isolates  
287 (Supplementary Fig. 15). Accessions carrying either the 7A resistance alone or both the 7A  
288 resistance and *Rwt3* showed similar level of resistance to both Br48 and Br48+*PWT3*.

289

### 290 **Acknowledgements**

291 The high-performance computing resources and services used in this work were supported by  
292 the Norwich Bioscience Institutes Partnership (NBIP) Computing infrastructure for Science  
293 (CiS) group alongside the Earlham Institute (EI) scientific computing group. We are grateful  
294 to the John Innes Centre (JIC) Horticultural Services for plant husbandry; EI for providing  
295 open access to the Kronos genome. This research was financed by the Biotechnology and  
296 Biological Sciences Research Council (BBSRC) Designing Future Wheat Cross-Institute

297 Strategic Programme to BBHW and PN (BBS/E/J/000PR9780); a John Innes Centre Institute  
298 Strategic Grant to BW; Science, Technology & Innovation Funding Authority (STDF),  
299 Egypt-UK Newton-Mosharafa Institutional Links award, Project ID (30718) to AFE and  
300 BBHW; the Gordon and Betty Moore Foundation through grant GBMF4725 to the Two  
301 Blades Foundation; and the Gatsby Charitable Foundation to JDGJ; National Science  
302 Foundation (Award#1943155) and USDA NIFA (Award#2020-67013-32558 and 2020-  
303 67013-31460) to NR and VT; European Research Commission grant (ERC-2016-STG-  
304 716233-MIREDI) to KVK and BBSRC Norwich Research Park Doctoral Training Grant  
305 (BB/M011216/1) for supporting EB.

### 306 **Author contributions**

307 This work was conceived by PN, JC and BBHW. Watkins panel configuration, DNA  
308 extraction and sequence acquisition (BBHW, LW, MFM, RA, SA, GY, AFE, JDGJ). Bait  
309 library design (KVK, EB, BS), *k*-mer matrix construction and association mapping (SA, KG),  
310 candidate genes discovery and analysis (SA, KG), Phylogenetic analysis (SA, KG), Blast  
311 isolates (YT, SAs), Phenotyping of diversity panels and TILLING mutants (AS, RG, TH, PN,  
312 CC, MHN), KASP marker design and analysis (SA, AS, KG, PN), Jagger mutants  
313 identification (VT, ASc, NR), Mutant confirmation and segregation (AS, RG, PN), cDNA  
314 RenSeq data (SA, AFE), Drafted manuscript (SA, PN, KG, RG, AS, VT, YT, ASc, NR, KK)  
315 and designed figures (SA, PN, KG, RG, AS, ASc, LW).

### 316 **Competing interests**

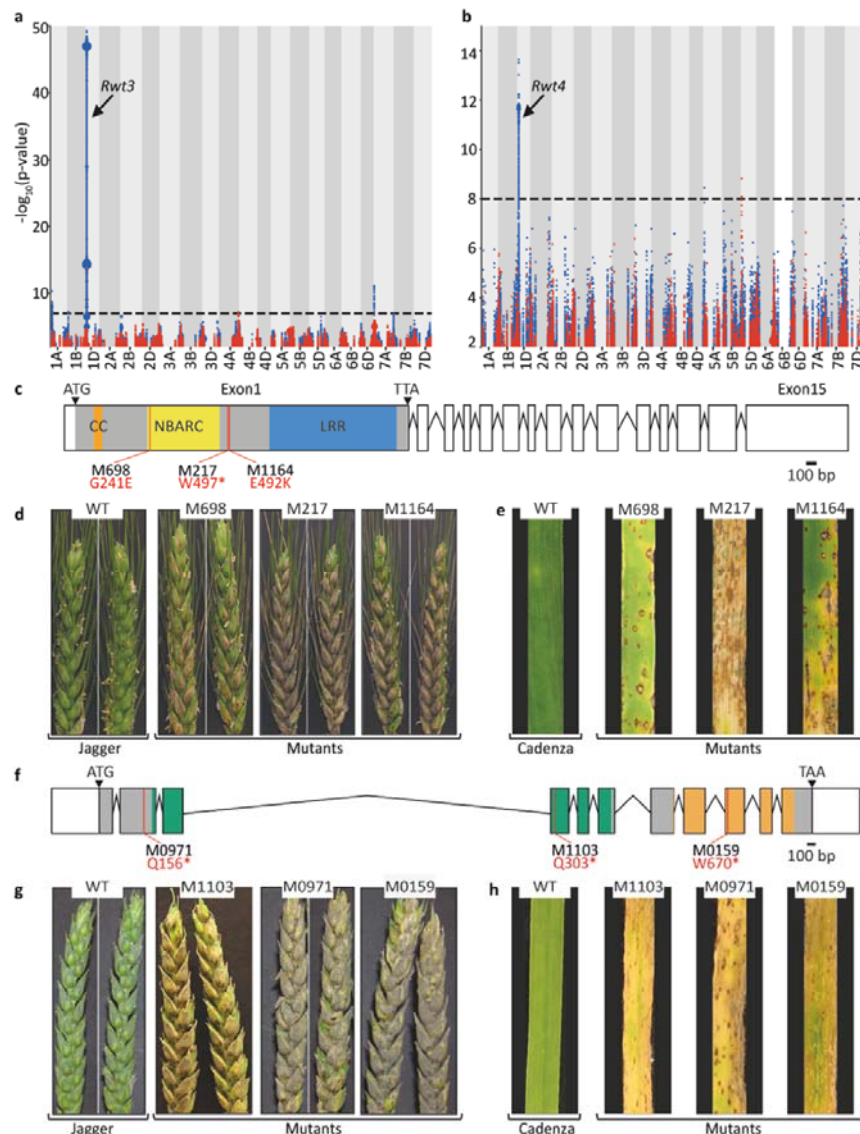
317 The authors declare no competing interests.

318

319

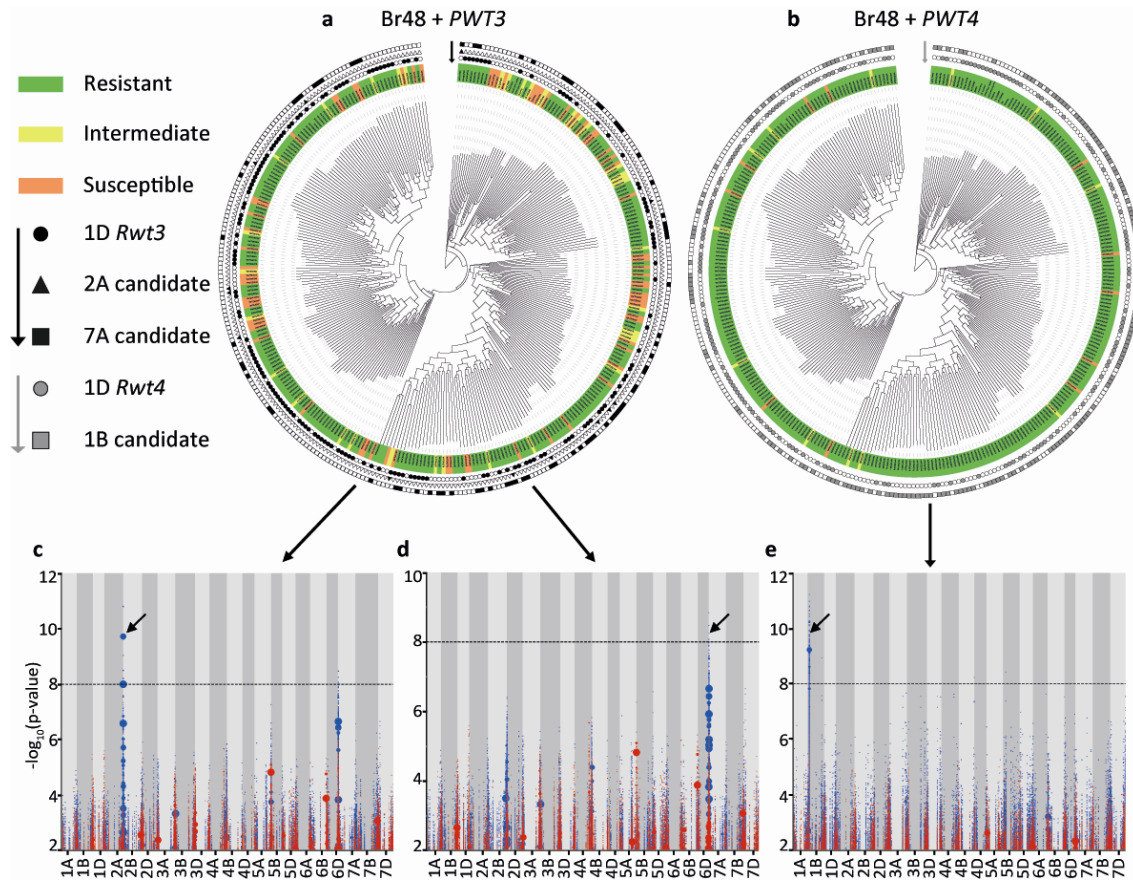
320

321



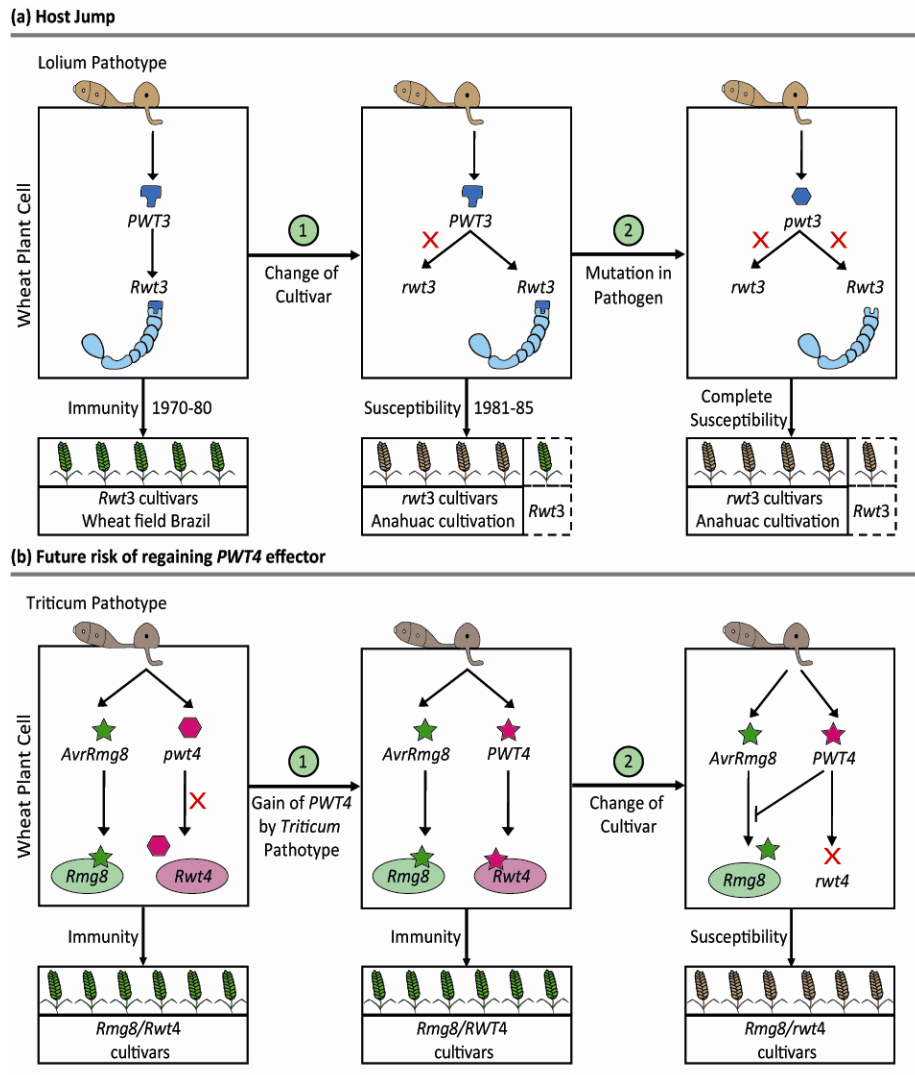
322

323 **Figure 1 | Genetic identification of the candidate genes recognising host-specific**  
324 **avirulence effectors of the blast fungus by *k*-mer-based association mapping on an *R*-**  
325 **gene enriched sequencing panel of wheat landraces. *k*-mers associated with resistance to**  
326 **(a) Br48+*Pwt3* mapped to Chinese Spring, and (b) Br48+*Pwt4* mapped to Jagger. Points on**  
327 **the y-axis depict *k*-mers positively associated with resistance in blue and negatively**  
328 **associated with resistance in red. Point size is proportional to the number of *k*-mers. (c)**  
329 **Structure of the NLR candidate gene for *Rwt3*. The predicted 1069 amino acids protein has**  
330 **domains with homology to a coiled-coil (CC), nucleotide-binding (NBARC) and leucine-rich**  
331 **repeats (LRR). Wheat blast (d) head and (e) detached leaf assays for the *Rwt3* Jagger mutants**  
332 **and wild type with Br48+*PWT3*. (f) Structure of the candidate gene for *Rwt4*. The predicted**  
333 **protein of 916 amino acids has domains with homology to a wheat tandem kinase (shown**  
334 **with green and orange colors). Wheat blast (g) head and (h) detached leaf assays for the *Rwt4***  
335 **Cadenza mutants and wild type with Br48+*PWT4*.**



336

337 **Figure 2 | Additional resistances to blast fungus and their distribution in the diversity**  
338 **panel of wheat landraces. (a)-(b) *k*-mer-based phylogeny of wheat landraces showing the**  
339 **phenotype of an accession after inoculation with: (a) Br48+*Pwt3* and (b) Br48+*Pwt4*, and the**  
340 **presence of the respective candidate resistance genes. Phenotype of an accession after**  
341 **inoculation with a blast isolate is indicated by the color used to highlight the label of that**  
342 **accession, while the presence and absence of allele-specific polymorphisms is indicated by**  
343 **filled symbols with black/grey or white, respectively. *k*-mers significantly associated with**  
344 **resistance to Br48+*Pwt3* in the absence of the *Rwt3* candidate gene on chromosome 1D leads**  
345 **to the identification of a resistance on (c) chromosome 2A when mapped to the assembly of**  
346 **wheat cultivar SY Mattis, and (d) chromosome 7A when mapped to wheat cultivar Jagger. (e)**  
347 ***k*-mers significantly associated with resistance to Br48+*Pwt4* in the absence of *Rwt4* candidate**  
348 **gene on chromosome 1D leads to the identification of a resistance on a region of chromosome**  
349 **1B containing the homeologue of *Rwt4*.**



350

351 **Figure 3 | A possible working model of host jump of blast fungus from *Lolium* to wheat**  
 352 **and a future risk associated with the reacquisition of *PWT4*.** (a) (i) A schematically drawn  
 353 wheat cell of a cultivar carrying *Rwt3* attacked by a *Lolium* isolate of the blast fungus. The  
 354 *PWT3* effector is recognized by *Rwt3* thus preventing the *Lolium* isolate from infecting  
 355 wheat. (ii) Widespread cultivation of cultivars lacking *Rwt3* (or having the susceptible allele,  
 356 *rwt3*) allowed the *Lolium* isolate to colonize wheat. (iii) The colonizing blast population  
 357 further expanded the host range by losing *PWT3* (or gaining the non-interacting effector,  
 358 *pwt3*) through mutation or recombination. (b) (i) A schematically drawn wheat cell of a  
 359 cultivar carrying *Rmg8* and *Rwt4* attacked by a *Triticum* isolate carrying *AvrRmg8*. The  
 360 *AvrRmg8* effector is recognized by *Rmg8*, thus preventing *Triticum* isolate from infecting the  
 361 cultivar. (ii) Gain of *Triticum* isolates gain the *PWT4* effector due to a future host jump but  
 362 are still not able to infect the cultivars carrying *Rwt4* (iii) However, cultivars lacking *Rwt4* (or  
 363 having the susceptible allele, *rwt4*) will be susceptible to the *Triticum* isolate carrying both  
 364 *AvrRmg8* and *PWT4* even if the cultivar carries *Rmg8* because in the absence of *Rwt4*, *PWT4*  
 365 suppresses the recognition of *AvrRmg8* by *Rmg8*. Therefore, the *Triticum* pathotype will be  
 366 able to further expand its host range.



367 **References**

- 368 1. Panstruga, R. & Moscou, M. J. What is the molecular basis of nonhost resistance? *Mol.*  
369 *Plant-Microbe Interact.* **33**, 1253–1264 (2020).
- 370 2. Igarashi S, Utiamada C M, Igarashi L C, Kazuma A H, L. R. S. Pyricularia in wheat: 1.  
371 Occurrence of Pyricularia sp. in Parana State. *Fitopatol Bras* **11**, 351–352 (1986).
- 372 3. Cruz, C. D. & Valent, B. Wheat blast disease: danger on the move. *Trop. Plant Pathol.*  
373 **42**, 210–222 (2017).
- 374 4. Malaker, P. K. *et al.* First Report of Wheat Blast Caused by Magnaporthe oryzae  
375 Pathotype triticum in Bangladesh. *Plant Dis.* **100**, 2330 (2016).
- 376 5. Tembo, B. *et al.* Detection and characterization of fungus (Magnaporthe oryzae  
377 pathotype Triticum) causing wheat blast disease on rain-fed grown wheat (Triticum  
378 aestivum L.) in Zambia. *PLoS One* **15**, e0238724 (2020).
- 379 6. Singh, P. K. *et al.* Wheat Blast: A Disease Spreading by Intercontinental Jumps and Its  
380 Management Strategies. *Front. Plant Sci.* **12**, 1467 (2021).
- 381 7. Inoue, Y. *et al.* Evolution of the wheat blast fungus through functional losses in a host  
382 specificity determinant. *Science (80-. ).* **357**, 80–83 (2017).
- 383 8. Takabayashi, N., Tosa, Y., Oh, H. S. & Mayama, S. A Gene-for-Gene Relationship  
384 Underlying the Species-Specific Parasitism of Avena/Triticum Isolates of  
385 Magnaporthe grisea on Wheat Cultivars.  
386 <http://dx.doi.org/10.1094/PHTO.2002.92.11.1182> **92**, 1182–1188 (2007).
- 387 9. Vy, T. T. P. *et al.* Genetic analysis of host-pathogen incompatibility between Lolium  
388 isolates of Pyricularia oryzae and wheat. *J. Gen. Plant Pathol.* **80**, 59–65 (2014).
- 389 10. Rush MC, Lindberg GD, C. R. BLAST-SERIOUS NEW DISEASE OF FORAGE  
390 GRASSES IN LOUISIANA. *Phytopathology* **62**, 806 (1972).
- 391 11. Farman, M. *et al.* The lolium pathotype of Magnaporthe oryzae recovered from a  
392 single blasted wheat plant in the United States. *Plant Dis.* **101**, 684–692 (2017).



- 393 12. Hirata, K., Tosa, Y., Nakayashiki, H. & Mayama, S. Significance of PWT4-Rwt4  
394 interaction in the species specificity of *Avena* isolates of *Magnaporthe oryzae* on  
395 wheat. *J. Gen. Plant Pathol.* **71**, 340–344 (2005).
- 396 13. Arora, S. *et al.* Resistance gene cloning from a wild crop relative by sequence capture  
397 and association genetics. *Nat. Biotechnol.* *2019 372* **37**, 139–143 (2019).
- 398 14. Gaurav, K. *et al.* Population genomic analysis of *Aegilops tauschii* identifies targets  
399 for bread wheat improvement. *Nat. Biotechnol.* *2021 1–10* (2021).  
400 doi:10.1038/s41587-021-01058-4
- 401 15. Rawat, N. *et al.* A TILLING Resource for Hard Red Winter Wheat Variety Jagger.  
402 *Crop Sci.* **59**, 1666–1671 (2019).
- 403 16. Lu, P. *et al.* A rare gain of function mutation in a wheat tandem kinase confers  
404 resistance to powdery mildew. *Nat. Commun.* *2020 111* **11**, 1–11 (2020).
- 405 17. Krasileva, K. V. *et al.* Uncovering hidden variation in polyploid wheat. *Proc. Natl.*  
406 *Acad. Sci. U. S. A.* **114**, E913–E921 (2017).
- 407 18. Zhan, S. W., Mayama, S. & Tosa, Y. Identification of two genes for resistance to  
408 *Triticum* isolates of *Magnaporthe oryzae* in wheat. *Genome* **51**, 216–221 (2008).
- 409 19. Tagle, A. G., Chuma, I. & Tosa, Y. Rmg7, a New Gene for Resistance to *Triticum*  
410 Isolates of *Pyricularia oryzae* Identified in Tetraploid Wheat. *Phytopathology* **105**,  
411 495–499 (2015).
- 412 20. Inoue, Y., Vy, T. T. P., Tani, D. & Tosa, Y. Suppression of wheat blast resistance by  
413 an effector of *Pyricularia oryzae* is counteracted by a host specificity resistance gene in  
414 wheat. *New Phytol.* **229**, 488–500 (2021).
- 415 21. Anh, V. L. *et al.* Rmg8, a new gene for resistance to *Triticum* isolates of *Pyricularia*  
416 *oryzae* in hexaploid wheat. *Phytopathology* **105**, 1568–1572 (2015).
- 417 22. Wingen, L. U. *et al.* Establishing the A. E. Watkins landrace cultivar collection as a  
418 resource for systematic gene discovery in bread wheat. *Theor. Appl. Genet.* **127**, 1831–  
419 1842 (2014).

- 420 23. Yu, G., Hatta, A., Periyannan, S., Lagudah, E. & Wulff, B. B. H. Isolation of Wheat  
421 Genomic DNA for Gene Mapping and Cloning. *Methods Mol. Biol.* **1659**, 207–213  
422 (2017).
- 423 24. Goddard, R. *et al.* Dissecting the genetic basis of wheat blast resistance in the  
424 Brazilian wheat cultivar BR 18-Terena. *BMC Plant Biol.* **20**, 1–15 (2020).
- 425 25. Marcussen, T. *et al.* Ancient hybridizations among the ancestral genomes of bread  
426 wheat. *Science (80-. )*. **345**, (2014).
- 427 26. Steuernagel, B., Witek, K., Jones, J. D. G. & Wulff, B. B. H. MutRenSeq: A Method  
428 for Rapid Cloning of Plant Disease Resistance Genes. *Methods Mol. Biol.* **1659**, 215–  
429 229 (2017).
- 430 27. Bolger, A. M., Lohse, M. & Usadel, B. Trimmomatic: a flexible trimmer for Illumina  
431 sequence data. *Bioinformatics* **30**, 2114–2120 (2014).
- 432 28. Marçais, G. & Kingsford, C. A fast, lock-free approach for efficient parallel counting  
433 of occurrences of k-mers. *Bioinformatics* **27**, 764–770 (2011).
- 434 29. International Wheat Genome Sequencing Consortium (IWGSC), T. I. W. G. S. C. *et*  
435 *al.* Shifting the limits in wheat research and breeding using a fully annotated reference  
436 genome. *Science* **361**, eaar7191 (2018).
- 437 30. Walkowiak, S. *et al.* Multiple wheat genomes reveal global variation in modern  
438 breeding. *Nat. 2020 5887837* **588**, 277–283 (2020).
- 439 31. Zhou, Y. *et al.* Introgressing the *Aegilops tauschii* genome into wheat as a basis for  
440 cereal improvement. *Nat. Plants 2021 76 7*, 774–786 (2021).
- 441 32. Steuernagel, B. *et al.* The NLR-Annotator Tool Enables Annotation of the Intracellular  
442 Immune Receptor Repertoire. *Plant Physiol.* **183**, 468–482 (2020).
- 443 33. Choi, Y., Sims, G. E., Murphy, S., Miller, J. R. & Chan, A. P. Predicting the functional  
444 effect of amino acid substitutions and indels. *PLoS One* **7**, (2012).